J Eng Math (2007) 57:365–379
DOI 10.1007/s10665-006-9049-y

ORIGINAL PAPER

Suppression of motion-induced residual longitudinal vibration of an elastic rod by input shaping

T.-S. Yang · K.-S. Chen · C.-C. Lee · I. Hu

Received: 14 June 2005 / Accepted: 28 March 2006 / Published online: 17 August 2006

Abstract Various input-shaping schemes such as the "zero-vibration" (ZV), "zero-vibration-and-derivative" (ZVD), "negative ZV" (NZV), and "negative ZVD" (NZVD) schemes have previously been proposed to suppress motion-induced residual vibration of lightly damped structures. In such schemes, the *input* command of the dynamical system in question is properly administered (i.e., *shaped*), so that the dominant induced vibration modes are annihilated through destructive interference. Here we are concerned with the effects of system payload on the vibration reduction capabilities of the aforementioned input-shaping schemes, especially when they are applied to continuous systems. By use of the simple structure of a linearly elastic rod as a specific example, it is demonstrated that both the minimum achievable residual vibration amplitude and the tolerance of detuning parameter errors of the input-shaping schemes are sensitive to the amount of payload on the system. It is therefore imperative to take the factor of system payload into account in the design of practical input shapers.

Keywords Elastic rod · Input shaping · Payload · Residual vibration suppression

1 Introduction

Movement of precision machine members and mechanical structures generally induces residual vibration that would deteriorate the performance of such systems. Usually the residual vibration can be suppressed by passive and/or active damping enhancement techniques [1, Chapters 3 and 6]. However, when it is impractical to implement sufficient damping on the system in question, one would have to resort to "input shaping" in order to suppress the undesirable residual vibration [2, 3].

Basically, the idea of input shaping is to decompose the input command of the system into a series of "partial commands", each applied at a proper instant, so that the residual vibration components induced by all partial commands interact destructively, thereby suppressing the overall residual vibration of the

T.-S. Yang (✉) · K.-S. Chen · C.-C. Lee · I. Hu
Department of Mechanical Engineering, National Cheng Kung University,
1 University Road, Tainan, Taiwan 701, R.O.C.
e-mail: tsyang@mail.ncku.edu.tw

system. (Of course, the trade-off here is the longer time required to complete the task, as there would be a series of time-delayed partial commands.) During the past 10 years or so, extensive research on input shaping has been conducted in robotics and flexible-arm control (see, for example, [2–10], and references cited therein). In such studies, the system dynamics typically is modeled by linearized equations of motion having single or low degrees of freedom, and input-shaping schemes resulting in "zero vibration" (ZV) and "zero vibration and derivative" (ZVD) are developed based on linear discrete models. Briefly, when the detuning (time lag) parameter value of the ZV scheme is correctly set, the residual vibration amplitude becomes zero. The ZVD scheme has the additional property that both the vibration amplitude itself and the derivative of the vibration amplitude with respect to the detuning parameter become zero simultaneously at the correct detuning parameter value. This means that, when the detuning parameter slightly deviates from its correct value (due to system aging or modeling errors, for example), the resulting residual vibration amplitude would still remain tolerably small. This nice property has rendered the ZVD scheme the preferable choice in practice [7, 11].

As it usually is also desirable to minimize the temporal duration of shaped input commands without much sacrifice of their detuning parameter error tolerance, "negative ZV" (NZV) and "negative ZVD" (NZVD) schemes—consisting of both positive and negative intermediate steps—have been derived [7], and successfully applied to minimize the residual and transient vibration amplitudes of gantry cranes [9]. In subsequent sections, we shall demonstrate that, for systems having single degree of freedom (SDOF), the NZV and NZVD schemes not only have significantly shorter input-command durations than that of the ZV and ZVD schemes, but also are nearly as tolerant of detuning parameter errors as the ZV and ZVD schemes, respectively.

To clarify the performance characteristics of various input-shaping schemes on nonlinear continuous systems (e.g., microelectromechanical [12] and nonlinear-wave [13, 14] systems), we have carried out a series of investigations along two complementary directions. First, to focus on the effects of system nonlinearities, Yang et al. [15] considered nonlinear SDOF systems. For such systems, the idea of suppressing residual vibration by exploiting linear destructive interference is no longer applicable. Alternatively, Yang et al. [15] interpreted input-shaping from an energy viewpoint, and proposed an efficient methodology of input-shaping design for nonlinear SDOF systems on the basis of an energy balance. The energy approach has also been successfully applied to design input shapers for an electromagnetically actuated nonlinear structure [15].

Meanwhile, along the other direction, we have studied input shaping for linear continuous structures, where there exist an infinite number of vibration modes in principle. Using as a particular example the model system of a cantilever beam driven by its base displacement, we have rigorously discussed the design methodology of input-shaping schemes from first principles [11]. Especially, the ZV and ZVD schemes originally proposed for discrete systems are employed to suppress the dominant vibration modes of the cantilever beam. The theoretical calculations have also been verified in an experimental study [16]. Generally speaking, when applied to continuous systems, the ZV and ZVD schemes do not produce zero residual vibration amplitude, due to the presence of the infinitely many other unsuppressed vibration modes. But as all modes are reduced in amplitude, the overall residual vibration amplitude still is smaller than that without input shaping.

Here, we shall march one step further, and examine the effects of system payload on the performance characteristics—especially the minimum achievable residual vibration amplitude and the tolerance of detuning parameter errors—of the ZV, ZVD, NZV, and NZVD input-shaping schemes when they are applied to continuous systems. In order to address this issue without undue analytical technicalities, we shall use the specific example of an elastic rod whose base is to be displaced by a prescribed distance. The issue is of practical interest because system payload generally would alter the spectrum (i.e., distribution of natural vibration frequencies) of the structure. So, unless the input-shaping schemes are tuned accordingly, their vibration-reduction capabilities would deteriorate in the presence of system payload. The system payload factor therefore must be taken into account in the design of practical input shapers. Moreover, we shall

also demonstrate that, although the NZV and NZVD schemes work well on SDOF systems, they may not be as attractive on continuous systems, in which some of the infinitely many unsuppressed vibration modes may actually be amplified, resulting in increased overall vibration amplitude.

The remainder of this paper is organized as follows: The mathematical problem is formulated and solved analytically (using the Laplace transform) for a unit-step base movement in Sect. 2. Then, in each of Sects. 3–6 we shall explain the basic ideas of the ZV, ZVD, NZV, and NZVD input-shaping schemes, respectively. Furthermore, from the system response to a unit-step input, the system response to each of the above input-shaping schemes is constructed by superposition, and then used to evaluate the performance characteristics of each input-shaping scheme. In particular, the effects of system payload on the performance characteristics of these schemes are examined. Also, to conclude this paper, a summary will be given in Sect. 7.

2 Formulation and system response to unit-step input

Consider an elastic rod of uniform cross-sectional area A; its material density and Young's modulus are ρ and E, respectively. The base of the rod is to be displaced by a distance H in a prescribed manner. Also, a point mass M (modeling the payload of the system) is attached to the tip of the rod. Dimensionless variables will be used throughout this paper, using the length of the rod L and maximum base displacement H, respectively, to scale the longitudinal position and local displacement of the rod. Meanwhile, the characteristic time scale is chosen to be L/c_0, where $c_0 = \sqrt{E/\rho}$ is the speed of linear wave propagation on the rod.

The motion of the rod therefore can be formulated as follows:

$$u_{tt} = u_{xx} \quad (0 < x < 1); \tag{1}$$

$$u = 0 = u_t \quad (t = 0), \tag{2}$$

$$u = f(t) \quad (x = 0), \tag{3}$$

$$u_x = -m\,u_{tt} \quad (x = 1). \tag{4}$$

Here x and t are the longitudinal coordinate and time, respectively, $u(x, t)$ is the local (longitudinal) displacement of the rod, and subscripts denote partial derivatives. Note also that, according to our normalization scheme, the base movement $f(t)$ appearing in (3) varies from zero at $t = 0$ to unity at a later instant in a prescribed manner. Meanwhile, in the tip boundary condition (4), the dimensionless parameter $m = M/\rho AL$ clearly is the ratio between the mass of the payload to that of the rod.

The mechanical system set-up given above actually has a broad range of practical applications. For example, in active mass-damper (AMD) systems that are widely used to reduce the vibration of tall buildings during strong winds or small earthquakes, a sufficiently large moving mass may be driven by a hydraulic actuator, which essentially is an elastic rod subjected to controlled base displacement (or force) [17]. When the base of the rod is displaced as programmed, the mass will move accordingly and exert a proper counterforce (due to its inertia) upon the building (to which the moving mass somehow is connected), and hence reduce the vibration amplitude of the building. An additional example of the practical application of our rod-mass model system is the suppression of residual vibration in high-rise elevators [18]. In such systems, the elevator car may be modeled as a rigid body (point mass) connected by flexible cables (which may be modeled as elastic rods; but of course, in elevator modeling the cables can only exert a tensile force upon the elevator car). For both of the above examples and our model system, the goal is to control precisely the motion of the mass.

It is also interesting to note that, as the above model problem is quite simple, similar problems have been analyzed and documented in the literature. For example, in the classical book of Timoshenko et al.

[19, Sect. 5.5], the problem of an elastic rod with a mass and/or spring attached at its end, and subjected to nonstationary stress loading is analyzed by use of a normal-mode method. The present work therefore has nothing to do with system complexities or new analytical techniques for vibration problems in engineering. As pointed out in the introduction, however, what we shall do in this work is to use the model problem formulated above as a vehicle for illustrating the basic ideas of various input-shaping schemes that are effective engineering tools for reducing motion-induced residual vibration of elastic structures. Moreover, we wish to evaluate carefully the effects of system payload (the tip mass here) on the performance characteristics of such input-shaping schemes.

Let us now turn to the solution of the model problem described by (1)–(4). For a unit-step input $f(t) = H(t)$, where $H(t)$ is Heaviside's step function, the system response can be readily obtained by use of the Laplace transform. Specifically, let us write

$$U(x,s) = \int_0^\infty \mathrm{e}^{-st} u(x,t)\,\mathrm{d}t$$

and, with the initial conditions (2), transform (1) into

$$U_{xx} = s^2 U. \tag{5}$$

Also, for the unit-step input, the boundary conditions (3) and (4) convert into

$$U = 1/s \quad (x = 0), \tag{6}$$

$$U_x = -ms^2 U \quad (x = 1). \tag{7}$$

The boundary-value problem posed by (5)–(7) can then readily be solved, yielding

$$U = \frac{\cosh s(x-1) - ms\sinh s(x-1)}{s(\cosh s + ms\sinh s)}. \tag{8}$$

We shall focus on the tip movement of the rod. So, let us set $x = 1$ in (8) and obtain

$$U(1,s) = s^{-1}(\cosh s + ms\sinh s)^{-1},$$

which has simple-pole singularities at $s = 0$ and $\pm\mathrm{i}\sigma_n$ ($n = 1,2,3,\ldots$), σ_n being the positive roots (ordered so that $0 < \sigma_1 < \sigma_2 < \cdots$) of the characteristic equation

$$\cos\sigma - m\sigma\sin\sigma = 0. \tag{9}$$

The corresponding residues are also calculated to be 1 at $s = 0$ and $-\{\sigma_n \sin\sigma_n(1 + m + m^2\sigma_n^2)\}^{-1}$ at both of the $s = \pm\mathrm{i}\sigma_n$ pair of poles.

Taking then the inverse transform

$$u(1,t) = \frac{1}{2\pi\mathrm{i}}\int_{0^+-\mathrm{i}\infty}^{0^++\mathrm{i}\infty} \mathrm{e}^{st} U(1,s)\,\mathrm{d}s,$$

and evaluating the integral above by the residue theorem [20, Sect. 54], we obtain the tip movement of the rod in the time domain:

$$u(1,t) = 1 - \sum_{n=1}^{\infty} \frac{2\cos\sigma_n t}{(1 + m + m^2\sigma_n^2)\sigma_n \sin\sigma_n}. \tag{10}$$

It is clearly seen in (10) that the tip movement of the rod consists of a steady-state value of unity and an infinite number of oscillation components of angular frequencies σ_n ($n = 1,2,3,\ldots$). Generally the vibration frequencies have to be calculated numerically from the characteristic equation (9), and the payload parameter m determines how the oscillation frequencies are distributed. For the special case of zero system payload ($m = 0$), however, the oscillation frequencies are readily found from (9) to be $\sigma_n = (n - 1/2)\pi$. Figure 1 plots the distribution of the vibration frequencies for various values of the payload parameter

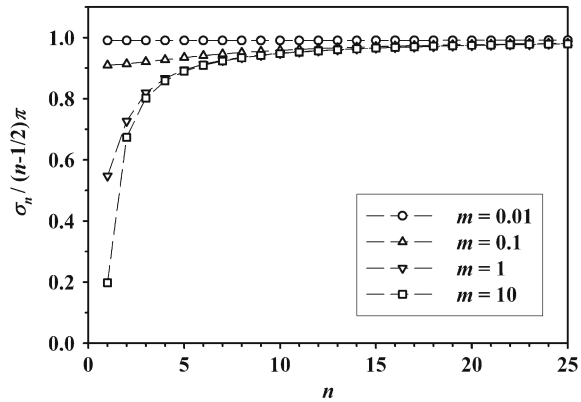

Fig. 1 Distribution of the vibration frequencies σ_n for various values of the payload parameter m. Plotted are the calculated vibration frequencies normalized by $(n - 1/2)\pi$, which are the vibration frequencies corresponding to $m = 0$

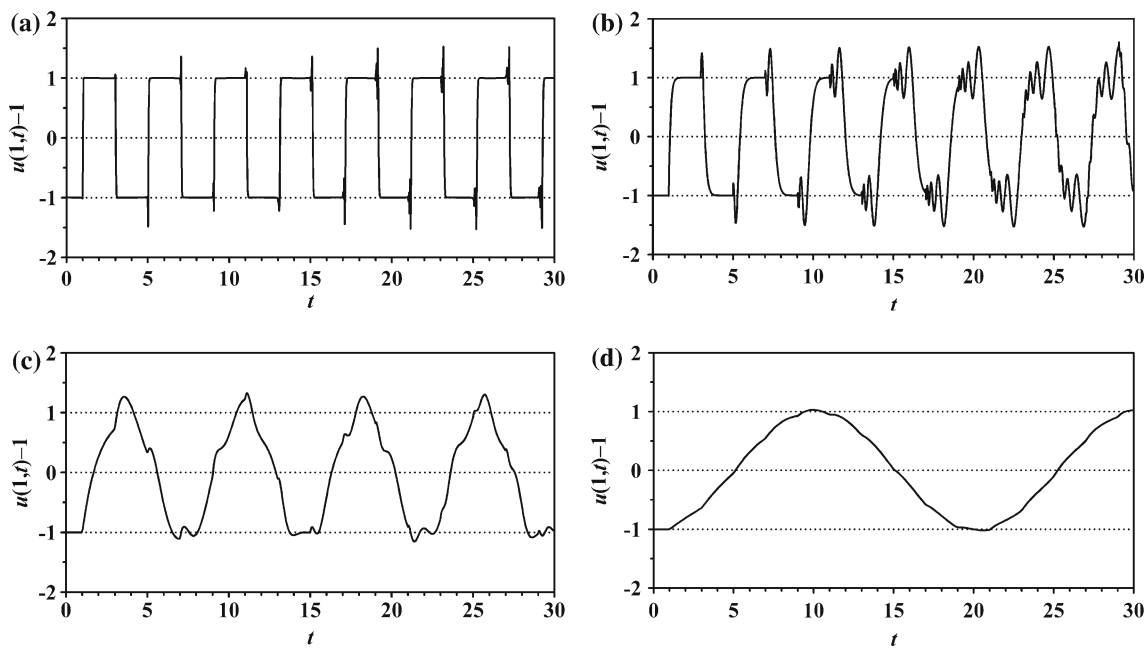

Fig. 2 Tip motion of an elastic rod excited by a unit-step base movement for (**a**) $m = 0{\cdot}01$, (**b**) $m = 0{\cdot}1$, (**c**) $m = 1$, and (**d**) $m = 10$

m. Generally speaking, increasing the value of m would decrease the corresponding vibration frequencies. Also, regardless of the value of m, for sufficiently large modal index n, it can be readily shown from (9) that $\sigma_n \sim n\pi$ $(n \to \infty)$.

After calculating the vibration frequencies, the tip movement of the rod due to a unit-step input can then be obtained from (10). Of course, in actual computations the total number of vibration components can only be finite, and here we take 128 components, so that relatively accurate results are obtained. The tip vibration is then sampled at the reasonably high rate of 128 data per period of the first vibration component $(2\pi/\sigma_1)$. Also, the tip movement of the rod is "watched" for 100 periods of the first vibration component, i.e., $100 \times 2\pi/\sigma_1$, so that the "maximum" amplitude of the residual tip vibration (relative to the mean position of the tip) can be determined accurately.

Tip movement of the rod thus calculated and recorded is plotted in Fig. 2 for various values of m. It is also interesting to note that for $m = 0$, the tip movement of the rod as described by (10) reduces to

$$u(1,t) = 1 + \sum_{n=1}^{\infty} \frac{4}{(2n-1)\pi} \sin\left[\left(n - \frac{1}{2}\right)\pi(t-1)\right],$$

which is simply the Fourier-series expansion of the "square wave"

$$2\sum_{n=0}^{\infty}(-1)^n H(t-2n-1).$$

The purely periodic system response results from the fact that for $m = 0$ the second and higher modal vibration frequencies are integral multiples of the fundamental frequency: $\sigma_n = (n - 1/2)\pi = (2n-1)\sigma_1$ for $n = 1, 2, 3, \ldots$. Generally speaking, when $m \neq 0$, the overall response of the tip deviates from the square-wave response for $m = 0$. Meanwhile, comparing Fig. 2a–d, we readily observe that the fundamental vibration period increases with the value of the payload parameter m, which is consistent with the results of natural frequencies plotted in Fig. 1. For sufficiently large values of m (e.g., $m = 10$), the system then becomes effectively SDOF, as is clearly seen in the resulting approximately sinusoidal tip motion shown in Fig. 2d.

Following the procedures described above, we can also calculate the maximum amplitude of the residual tip vibration excited by a unit-step input (i.e., base movement of the rod) for various values of the payload parameter m, and the results are plotted in Fig. 3. It appears that for $m \approx 0{\cdot}1$ the tip has the largest maximum residual vibration amplitude, as many vibration components are then making significant contributions to the resultant amplitude. Also, as m increases from there, the residual vibration amplitude decreases and asymptotes to unity, which can be readily shown to be the residual tip-vibration amplitude of the limiting SDOF system. As the value of m decreases from 0·1, however, the second and higher modal vibration frequencies become closer to integral multiples of the fundamental frequency, so that the overall system response becomes more purely periodic and the residual tip vibration decreases accordingly. Note also that, although the unity vibration amplitude of the square-wave response should be obtained as $m \to 0$, the residual vibration amplitude nevertheless fluctuates between 1 and about 1·2 as observed in Fig. 3. This seemingly random fluctuation of the residual vibration amplitude actually results from the well studied Gibbs phenomenon [21, Sect. 49], which arises when a discontinuous function (like the square wave here) is represented by a Fourier series. Specifically, as our procedure for determining the residual vibration amplitude described above samples a fixed number of data within a period, and over a fixed number of periods, sometimes it misses the maximum amplitude (about 1·2 in Fig. 3) of the fluctuation caused by the Gibbs phenomenon (which is not physical though). Of course, as we have checked, increasing both the number of watched periods and the number of data within each period would reduce the seemingly random nature of the results in Fig. 3 for small values of m. However, to stay focused, we will not present a more

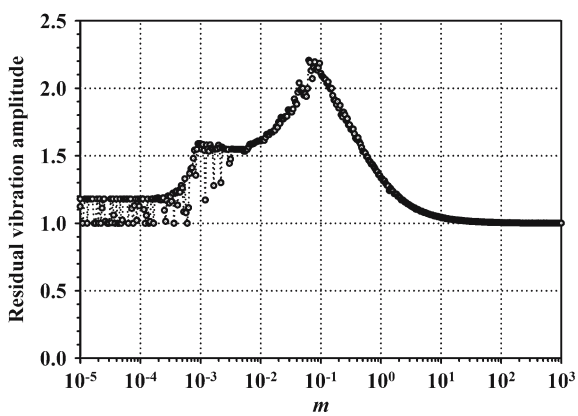

Fig. 3 Maximum amplitude of the residual tip vibration of an elastic rod excited by unit-step base movement, for various values of the payload parameter m

detailed discussion of the Gibbs phenomenon, and will go right on to discuss a number of input-shaping schemes for residual vibration suppression.

3 The ZV scheme

As the unit-step response (10) indicates, in the absence of damping the tip of the rod would never rest at the target position $u = 1$. One then has to resort to input shaping in order to suppress the tip vibration induced by the base movement of the rod, and here we shall explain the basic ideas of a number of input-shaping schemes, beginning in this section with the "zero-vibration" (ZV) scheme. Also, in the ensuing discussion let us try to suppress the first vibration frequency σ_1, as it typically contributes most to the overall tip vibration. The possibilities of suppressing a number of different frequencies simultaneously exist, and will also be briefly discussed.

Note first that the equation of motion (1) is linear and invariant with respect to time shift. The system response to an input $f(t)$ that consists of a series of intermediate steps therefore can be readily constructed from the unit-step response (10) by superposition. Specifically, suppose that the input is split into two partial steps of equal magnitude 1/2, and the second partial step is administered at $t = \tau$, i.e.,

$$f(t) = \frac{1}{2}\{H(t) + H(t-\tau)\}. \tag{11}$$

Then, the overall tip motion for $t > \tau$ (i.e., after the base of the rod has reached its destination) is

$$u(1,t) = 1 - \sum_{n=1}^{\infty} \frac{A_{n,\mathrm{ZV}} \cos\sigma_n(t-\tau/2)}{(1+m+m^2\sigma_n^2)\sigma_n \sin\sigma_n}, \tag{12}$$

where

$$A_{n,\mathrm{ZV}} = 2\cos\frac{\sigma_n\tau}{2}$$

are modal amplitude factors.

It then transpires that the amplitude of the nth vibration component (i.e., the component having angular frequency σ_n) is reduced by a factor of $|\cos(\sigma_n\tau/2)|$ when the two-step input-shaping scheme (11) is used instead of a unit-step input. In particular, when $\tau = \pi/\sigma_1$, the time delay of the second partial step is just one half of the period of the first vibration component, so that the first component is completely suppressed through destructive interference. The scheme (11) with the zero-vibration time delay $\tau = \pi/\sigma_1$ therefore is called the ZV scheme [7, 11].

Note, however, that, even when the first vibration component is completely suppressed, higher vibration components generally still would persist (but with reduced amplitude). Therefore, as seen in Fig. 4a, the overall tip-vibration amplitude of the rod is reduced but nonzero. [Both Fig. 4a, b show the dependence of residual vibration amplitude upon the payload parameter m (for different input-shaping schemes), and therefore are put together for comparison. The performance characteristics of other schemes will be discussed in due course.] An interesting special case occurs when there is no payload ($m = 0$), so that $\sigma_n = (n-1/2)\pi$ and hence $\tau = \pi/\sigma_1 = (2n-1)\pi/\sigma_n$ for all n. Accordingly, the correct time delay to trigger destructive interference for the first component would also suppress all higher components, resulting in complete suppression of the overall tip vibration of the rod. This is consistent with the observation in Fig. 4a that, as $m \to 0$, the residual vibration amplitude resulting from the ZV input command becomes extremely small.

For $m \neq 0$, however, more sophisticated input-shaping schemes have to be employed to suppress two or more vibration components simultaneously. For example, suppose that it is desirable to suppress the first and second vibration components at the same time, one may then convolve the ZV scheme for the first frequency with that for the second frequency, resulting in an input command of the form

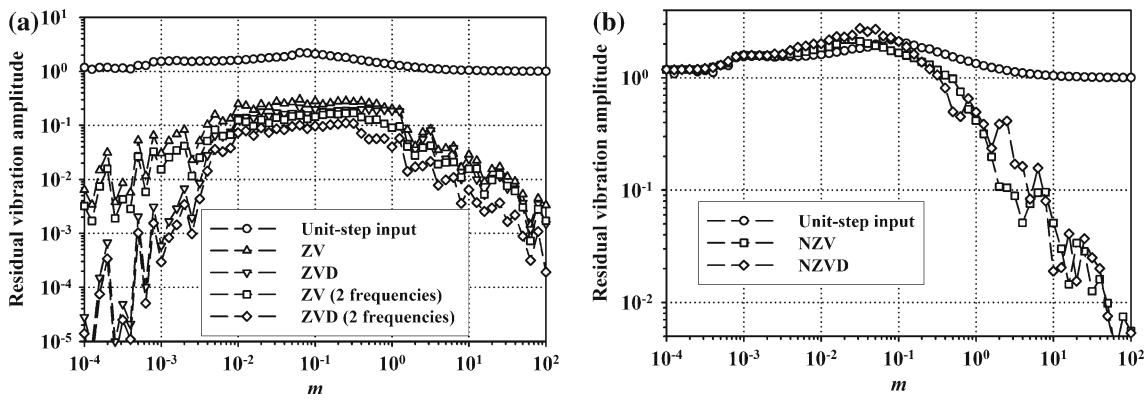

Fig. 4 Residual vibration amplitudes as functions of the payload parameter m, excited by (**a**) ZV and ZVD commands that suppress the first only or the first two vibration frequencies, and (**b**) NZV and NZVD commands suppressing the first frequency. The vibration amplitudes excited by a unit-step input are also plotted for comparison

$$f(t) = \frac{1}{2}\left\{\frac{1}{2}H(t) + \frac{1}{2}H(t-\tau_1)\right\} + \frac{1}{2}\left\{\frac{1}{2}H(t-\tau_2) + \frac{1}{2}H(t-\tau_1-\tau_2)\right\}$$
$$= \frac{1}{4}\left\{H(t) + H(t-\tau_2) + H(t-\tau_1) + H(t-\tau_1-\tau_2)\right\}, \tag{13}$$

where $\tau_1 = \pi/\sigma_1$ and $\tau_2 = \pi/\sigma_2$. As shown in Fig. 4a, for all values of the payload parameter m, when the above input command is employed, the overall residual vibration amplitude is even smaller than that excited by the single-frequency ZV scheme (11). Of course, the trade-off here is the longer time $\tau_1 + \tau_2$ required to complete the above input command (compared with τ_1 for the ZV command that suppresses the first frequency only). Input commands that simultaneously suppress more frequencies clearly can be composed in the same way, and are expected to further reduce the residual vibration amplitude.

Now let us examine the parameter-error tolerance of the ZV scheme, which is an important issue because practical mechanical systems more or less possess certain system-parameter uncertainties. For example, the actual vibration frequencies σ_n may differ from their nominal estimates $\sigma_{n,\text{nom}}$ due to system-modeling errors or aging of the system. Accordingly, if one determines the time-delay parameter in (11), using the first nominal frequency, i.e., $\tau = \pi/\sigma_{1,\text{nom}}$, attempting to suppress the first vibration frequency, then the vibration-reduction factor for the nth component is

$$\left|\frac{A_{n,\text{ZV}}(\tau)}{A_{n,\text{ZV}}(0)}\right| = \left|\cos\left(\frac{\pi}{2}\frac{\sigma_n}{\sigma_1}\delta\right)\right|,$$

which would not vanish, even for $n = 1$, unless the ratio of the actual frequency to the nominal frequency $\delta = \sigma_1/\sigma_{1,\text{nom}} = 1$ (i.e., when the input command is correctly tuned). A certain amount of residual vibration therefore would persist. On top of that, at the correct time delay corresponding to $\delta = 1$, the slope of the vibration-reduction factor with respect to the frequency ratio δ obtains its maximum value, meaning that a rather slight error in the time delay would result in a relatively significant amount of residual vibration (see Fig. 5). The attempt to improve the tolerance of detuning-parameter errors of the ZV scheme has led to the development of the "zero-vibration-and-derivative" (ZVD) scheme, to be discussed in the next section.

As here we are concerned with the effects of system payload on the overall system response (consisting of a large number of vibration frequencies) of the rod, we have also followed the procedures described earlier in Sect. 2 to record the maximum deviation of the tip displacement from the target position $u = 1$. The recorded maximum deviation is then taken to be the residual vibration amplitude, and is divided by the residual vibration amplitude excited by a unit-step input (see Fig. 3) to calculate the overall "residual vibration reduction factor" due to the specific input shaping scheme employed.

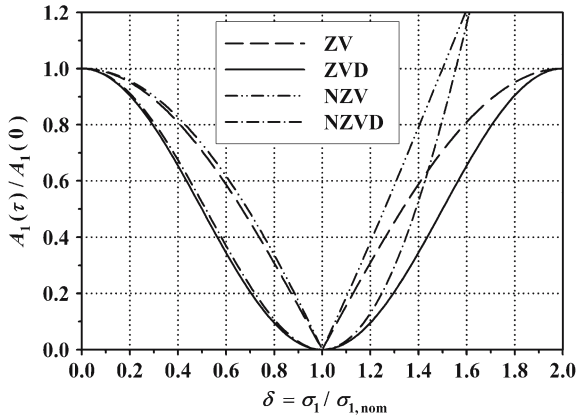

Fig. 5 Comparison of the parameter-error tolerance of the ZV, ZVD, NZV, and NZVD schemes. Here the amplitude-reduction factor for the first vibration component, $A_1(\tau)/A_1(0)$ with $\tau=\pi/\sigma_{1,\mathrm{nom}}$, is plotted as a function of the frequency-ratio parameter $\delta=\sigma_1/\sigma_{1,\mathrm{nom}}$

Figure 6a plots the residual vibration reduction factor resulting from the ZV scheme for various values of the payload parameter m. As explained above, for small nonzero m, due to the presence of unsuppressed residual vibration components of higher frequencies, the overall tip-vibration amplitude does not vanish at $\delta = \sigma_1/\sigma_{1,\mathrm{nom}} = 1$. Also, generally speaking, as the value of m increases from zero, the minimum achievable residual vibration-reduction factor first increases, because more of the higher vibration components survive from input shaping and make more contributions to the overall tip vibration of the rod. (Recall that for $m = 0$ an accurate input-shaping scheme suppresses all residual vibration frequencies simultaneously.) When m becomes sufficiently large, however, the minimum achievable residual vibration-reduction factor begins to decrease, as the system behaves more and more like a SDOF system for the input-shaping scheme to work effectively. Moreover, Fig. 6a also indicates that the ZV scheme's tolerance of the detuning (time

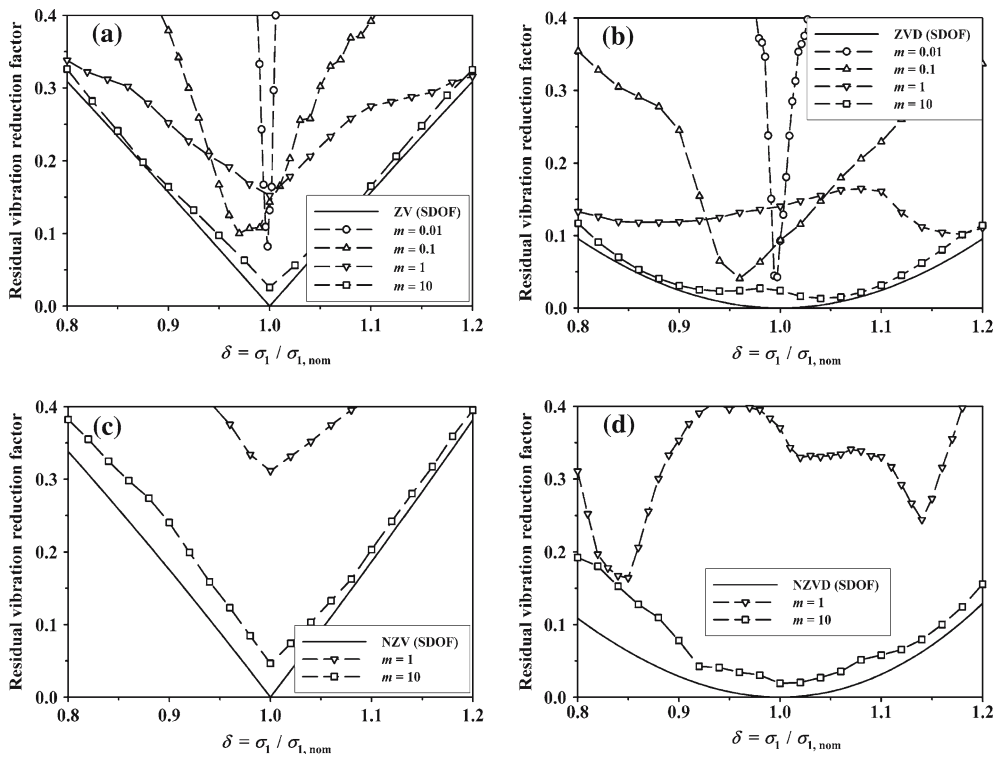

Fig. 6 Detuning-parameter error tolerance of the (**a**) ZV, (**b**) ZVD, (**c**) NZV, and (**d**) NZVD schemes for various values of the payload parameter m. The residual vibration-reduction factor is defined in the text

delay) parameter error increases with m. This is also related to the above interpretation that the system behaves more and more like a SDOF system as m increases.

4 The ZVD scheme

As pointed out above, in order to increase the detuning-parameter error tolerance of an input-shaping scheme, it is desirable to have zero derivative of the residual vibration amplitude with respect to the time delay when the vibration amplitude itself is zero (i.e., under a ZV condition). This adds one constraint to the design of an input-shaping scheme, and therefore can only be achieved with one more intermediate partial step than the ZV scheme (11). Technically, by considering three-step inputs where the three partial steps are equally separated in time and have magnitudes that add up to unity, one may deduce the correct partial-step magnitudes and time separation by requiring the residual vibration amplitude and its derivative with respect to the time separation to be zero simultaneously under ZV conditions. It can then be shown that the base movement of the rod has to be completed in the following manner:

$$f(t) = \frac{1}{4}\{H(t) + 2H(t-\tau) + H(t-2\tau)\}. \tag{14}$$

Accordingly, the overall tip motion for $t > 2\tau$ is calculated from the unit-step response (10) by superposition to be

$$u(1,t) = 1 - \sum_{n=1}^{\infty} \frac{A_{n,\mathrm{ZVD}} \cos\sigma_n(t-\tau)}{(1+m+m^2\sigma_n^2)\sigma_n \sin\sigma_n}, \tag{15}$$

where the modal amplitude factors are found to be

$$A_{n,\mathrm{ZVD}} = 2\cos^2\frac{\sigma_n\tau}{2}.$$

Clearly, the first vibration component (corresponding to $n = 1$) vanishes under the same ZV condition $\tau = \pi/\sigma_1$ for the ZV scheme, in which case the vibration components excited by first and last partial steps interact constructively and jointly annihilate the vibration component excited by the partial step in between. In this way the derivative of the vibration-reduction factor for the first vibration component

$$\frac{A_{1,\mathrm{ZVD}}(\tau)}{A_{1,\mathrm{ZVD}}(0)} = \cos^2\frac{\sigma_1\tau}{2}$$

with respect to the time-delay parameter τ would also vanish at $\tau = \pi/\sigma_1$. For this reason, the three-step input-shaping scheme (14) is called the "zero-vibration-and-derivative" (ZVD) scheme [7, 11]. Also, as illustrated in Fig. 5, this implies that, when the time-delay parameter is slightly off the correct ZV value (corresponding to $\delta = 1$ in Fig. 5), much smaller residual vibration of the first frequency (and hence smaller overall residual vibration, too) would be excited by the ZVD scheme than that excited by the ZV scheme.

Since the ZVD scheme is more tolerant of detuning-parameter errors than the ZV scheme, it is therefore the preferable scheme in practice. The price to pay here, however, is the longer command duration $2\pi/\sigma_1$ for the ZVD scheme than the duration π/σ_1 for the ZV scheme. Clearly, from a practical perspective, it will generally be desirable to minimize the command duration, while maintaining the detuning-parameter error tolerance of the ZVD scheme. This has led to the negative schemes to be discussed in the next two sections.

Meanwhile, we would like to point out that multi-frequency ZVD input commands can also be composed by convolution as was done for the ZV scheme in the previous section. To suppress two frequencies simultaneously in a ZVD manner, for example, one would need a total of nine partial steps. Specifically, the double ZVD scheme that suppress the first and second vibration frequencies simultaneously reads

$$f(t) = \frac{1}{4}\left\{\frac{1}{4}H(t) + \frac{1}{2}H(t-\tau_1) + \frac{1}{4}H(t-2\tau_1)\right\}$$
$$+ \frac{1}{2}\left\{\frac{1}{4}H(t-\tau_2) + \frac{1}{2}H(t-\tau_1-\tau_2) + \frac{1}{4}H(t-2\tau_1-\tau_2)\right\}$$
$$+ \frac{1}{4}\left\{\frac{1}{4}H(t-2\tau_2) + \frac{1}{2}H(t-\tau_1-2\tau_2) + \frac{1}{4}H(t-2\tau_1-2\tau_2)\right\}, \tag{16}$$

where, as before, $\tau_1 = \pi/\sigma_1$ and $\tau_2 = \pi/\sigma_2$. [Note also that the partial steps in (16) have not been correctly ordered in their application times.] Of course, input commands that suppress more frequencies simultaneously can be composed in the same manner.

As shown in Fig. 4a for each value of the payload parameter m, while the single-frequency ZVD scheme (14) already reduces the residual vibration amplitude significantly, the double-frequency ZVD scheme (16) can further reduce the residual vibration amplitude. Again, the trade-off here is the longer time $2\tau_1 + 2\tau_2$ required to complete the double-frequency ZVD input command (compared with $2\tau_1$ for the single-frequency ZVD command). Moreover, the results plotted in Fig. 4a also indicate that the overall residual vibration amplitude resulting from the ZVD input command generally is smaller than that from the ZV command. This is in fact easy to understand: since the ZVD command has a longer time duration and hence a narrower spectral content, consequently fewer higher-frequency vibration components are excited and contribute to the overall vibration amplitude. The dependence on the payload parameter m of the residual vibration amplitude resulting from the ZVD input command is qualitatively the same as that for the ZV command (see Sect. 3), so let us not repeat the physical interpretation of such dependence here.

We have also studied the detuning-parameter error tolerance of the ZVD scheme (14), and the results are shown in Fig. 6b for various values of the payload parameter m. Comparing Fig. 6a and b, we see that, when applied to a continuous rod that in principle has an infinite number of vibration components, the ZVD scheme still is more robust than the ZV scheme. Also, as already explained above, since the ZVD command excites fewer higher-frequency vibration components, the minimum achievable residual vibration reduction factor for the ZVD command is smaller than that for the ZV command. Moreover, the dependencies of the minimum achievable residual vibration reduction factor and the detuning-parameter error tolerance of the ZVD scheme on the payload parameter m are similar to those of the ZV scheme discussed in the previous section. In particular, as m becomes sufficiently large, the minimum achievable residual vibration reduction factor decreases, and the detuning parameter error tolerance improves, as the system behaves more and more like a SDOF system for the input shaping scheme to work effectively.

5 The NZV scheme

Suppose now that both positive and negative steps of unit magnitude are used. As an example, consider

$$f(t) = H(t) - H(t-\tau_1) + H(t-\tau_2), \tag{17}$$

where $0 < \tau_1 < \tau_2$. Note, in particular, that, as for both the ZV and ZVD schemes discussed above, the magnitudes of all the partial steps add up to unity, so that, when the input command is completed, the base of the rod undergoes a unit displacement. Also, using the unit-step response (10), the resulting tip movement of the rod is calculated by superposition to be

$$u(1,t) = 1 - \sum_{n=1}^{\infty} \frac{A_{n,\mathrm{NZV}} \cos(\sigma_n t - \phi_{n,\mathrm{NZV}})}{(1+m+m^2\sigma_n^2)\sigma_n \sin\sigma_n}, \tag{18}$$

where

$$A_{n,\mathrm{NZV}} = 2\{(1-\cos\sigma_n\tau_1+\cos\sigma_n\tau_2)^2 + (\sin\sigma_n\tau_1 - \sin\sigma_n\tau_2)^2\}^{1/2}$$

and

$$\phi_{n,\mathrm{NZV}} = \tan^{-1} \frac{\sin \sigma_n \tau_2 - \sin \sigma_n \tau_1}{1 - \cos \sigma_n \tau_1 + \cos \sigma_n \tau_2}.$$

Of course, the objective here is to choose the right values for the time-delay parameters $\tau_{1,2}$ so that the first vibration component (corresponding to $n = 1$) is suppressed. From the above expressions, it is clear that this occurs when $\sin \sigma_1 \tau_1 = \sin \sigma_1 \tau_2$ and $\cos \sigma_1 \tau_1 = -\cos \sigma_1 \tau_2 = 1/2$, i.e.,

$$\sigma_1 \tau_1 = \pi/3 \quad \text{and} \quad \sigma_1 \tau_2 = 2\pi/3.$$

With these ZV time delays, the input command (17) is called the "negative ZV" (NZV) scheme [7] (because a negative step is used). Note that placing the steps of alternating signs in (17) symmetrically with respect to the middle one is essential for suppressing the overall residual vibration. Also, when the best nominal estimate of the first vibration frequency $\sigma_{1,\mathrm{nom}}$ is used to calculate the time delay parameters so that $\tau_1 = \pi/3\sigma_{1,\mathrm{nom}}$ and $\tau_2 = 2\pi/3\sigma_{1,\mathrm{nom}}$, the resulting vibration-reduction factor for the first component is

$$\frac{A_{1,\mathrm{NZV}}(\tau)}{A_{1,\mathrm{NZV}}(0)} = \left| 1 - 2\cos\frac{\pi\delta}{3} \right|,$$

where $\delta = \sigma_1/\sigma_{1,\mathrm{nom}}$ is the ratio between the actual and nominal vibration frequencies as defined before.

Note that the total input-command duration of the (correctly tuned) NZV scheme is $\tau_2 = 2\pi/3\sigma_1$, and thus is 33% shorter than the ZV command duration π/σ_1. Nevertheless, as shown in Fig. 5, close to the ZV condition where $\delta = 1$ the robustness of the NZV scheme is nearly as good as the ZV scheme. It should also be noted, however, that, when the time-delay parameter is significantly wrong (when δ is greater than about 1·5; see Fig. 5), the resulting vibration amplitude can exceed that without input shaping. This has important consequences indeed when the NZV scheme is applied to continuous systems because, while the target residual vibration component (the first component here) is suppressed by the NZV scheme, other components may indeed be amplified, resulting in larger overall residual vibration amplitude.

As a matter of fact, the results shown in Fig. 4b indicate that, for smaller values of the payload parameter m (i.e., when a large number of vibration components are contributing significantly), the NZV scheme would excite a larger residual vibration amplitude than that excited by the unit-step input. The results of the parameter-error study shown in Fig. 6c also indicate that, in comparison with the results shown in Fig. 6a and b, the value of m has to be large enough in order for the rod to be approximately SDOF, and the NZV scheme to work satisfactorily. We thus conclude that, while the NZV scheme works properly and efficiently for approximately SDOF systems (corresponding here to large values of m), it may actually make things worse when applied to continuous systems in which a large number of vibration components participate significantly. Hence it appears to be pointless to suppress two or more vibration frequencies by convolving the NZV scheme as was done for the ZV and ZVD schemes.

6 The NZVD scheme

Now, with more alternating positive and negative unit steps, it is also possible to render both the resulting vibration amplitude and its derivative with respect to time delay zero simultaneously. Specifically, let us consider an input command that consists of five unit steps of alternating signs:

$$f(t) = H(t) - H(t-\tau_1) + H(t-\tau_2) - H(t-\tau_3) + H(t-\tau_4). \tag{19}$$

As we have seen in the discussion of the NZV scheme above, placing the alternating steps symmetrically with respect to the middle one is essential for suppressing the overall residual vibration. So, to simplify the calculation, we shall require *a priori* that

$$\tau_4 - \tau_2 = \tau_2 \quad \text{and} \quad \tau_3 - \tau_2 = \tau_2 - \tau_1,$$

i.e., $\tau_4 = \tau_1 + \tau_3 = 2\tau_2$. With such constraints, the resulting tip movement of the rod again is calculated by superposition, yielding

$$u(1,t) = 1 - \sum_{n=1}^{\infty} \frac{A_{n,\mathrm{NZV}} \cos\sigma_n(t-\tau_2)}{(1+m+m^2\sigma_n^2)\sigma_n \sin\sigma_n} \tag{20}$$

where

$$A_{n,\mathrm{NZVD}} = 2\{1 + 2\cos\sigma_n\tau_2 - 2\cos\sigma_n(\tau_2 - \tau_1)\}.$$

To suppress the nth residual vibration component in a ZVD manner, we require that $A_{n,\mathrm{NZVD}} = 0$ and $\partial A_{n,\mathrm{NZVD}}/\partial\sigma_n = 0$ simultaneously. The two resulting algebraic equations are then solved numerically, yielding

$$\sigma_n\tau_2 = 0{\cdot}732\pi, \quad \sigma_n(\tau_2 - \tau_1) = 0{\cdot}553\pi.$$

So, if the first vibration component is to be suppressed, the time-delay parameters in the "negative ZVD" (NZVD) scheme (19) must be chosen such that

$$\sigma_1\tau_1 = 0{\cdot}179\pi, \quad \sigma_1\tau_2 = 0{\cdot}732\pi, \quad \sigma_1\tau_3 = 1{\cdot}285\pi, \quad \sigma_1\tau_4 = 1{\cdot}464\pi.$$

Meanwhile, if the nominal estimate of the first vibration frequency $\sigma_{1,\mathrm{nom}}$ is used instead to calculate the time-delay parameters above, the resulting vibration-reduction factor for the first vibration component would be

$$\frac{A_{1,\mathrm{NZVD}}(\tau)}{A_{1,\mathrm{NZVD}}(0)} = 1 - 2\cos(0{\cdot}553\pi\delta) + 2\cos(0{\cdot}732\pi\delta),$$

where $\delta = \sigma_1/\sigma_{1,\mathrm{nom}}$ as already defined before. Note that the total duration of the NZVD command $\tau_4 = 1{\cdot}464\pi/\sigma_1$ is 27% shorter than the duration of the ZVD scheme $2\pi/\sigma_1$, while its robustness is nearly as good as the ZVD scheme close to the ZV condition where $\delta = \sigma_1/\sigma_{1,\mathrm{nom}} = 1$, as shown in Fig. 5. Like the NZV scheme, however, when the time-delay parameter is significantly wrong (when $\sigma_1/\sigma_{1,\mathrm{nom}}$ is greater than about 1·5), the resulting vibration amplitude can exceed that without input shaping. As demonstrated in Figs. 4b and 6d, this implies that the residual vibration amplitude resulting from the NZVD scheme actually becomes larger than that excited by the unit-step input for smaller values of the payload parameter m, and it takes a relatively large value of m for the system to be approximately SDOF and the NZVD scheme to work properly. Therefore, just like the NZV scheme, the NZVD scheme actually is not suitable for continuous systems.

7 Concluding remarks

In this paper, the simple system of a linearly elastic rod with a point mass attached at its tip, and subjected to controlled base displacement, is considered as a specific example for continuous elastic structures with payload. Despite its simplicity, the model system is closely related to a broad range of practical applications such as AMD systems [17] and high-rise elevators [18], as explained above. The goal here is to precisely control the motion of the mass. Although the present work does not involve new analytical techniques for vibration engineering problems, we have used the model problem as a vehicle for illustrating the basic ideas of various input-shaping schemes that are effective engineering tools for reducing motion-induced residual vibration of elastic structures, and carefully evaluated the effects of system payload on the performance characteristics of such input-shaping schemes.

Specifically, here we have explained the main ideas of the ZV, ZVD, NZV and NZVD input-shaping schemes. Basically, in the ZV scheme (11) the input command is split into two partial steps of equal magnitude (one half of the total stroke) and separated in time by one half of the period of the vibration

component to be suppressed. By doing so, we trigger linear destructive interference to annihilate the target vibration component. In order to increase the detuning (time delay) parameter error tolerance of the ZV scheme, the ZVD scheme (14) that consists of three partial steps is then devised. Also, the attempt to shorten the total input-command duration has led to the development of the negative input-shaping schemes, i.e., the NZV and NZVD schemes given by (17) and (19), respectively.

All the aforementioned input-shaping schemes have been devised with the purpose of suppressing a single dominant vibration frequency, although multi-frequency input-shaping schemes clearly can be constructed by convolution (as we have done for the ZV and ZVD schemes in Sects. 3 and 4, respectively). When applied to a continuous system like the elastic rod considered in this paper, however, the remaining higher components of residual vibration may or may not be reduced at the same time, and hence the overall residual vibration amplitude may or may not be reduced. In fact, as we have shown above, for smaller values of the system payload parameter m, more vibration components contribute significantly, while for larger values of m the system is essentially SDOF. Furthermore, while the amplitude of all residual vibration components are reduced by the positive (i.e., the ZV and ZVD) schemes, this is not the case for the negative (i.e., the NZV and NZVD) schemes. As a result, generally a large payload is required for the system to be approximately SDOF so that the negative schemes could work properly. This finding clearly should be taken into account in the design of practical input shapers.

The results of our examination on the detuning-parameter error tolerance of the input-shaping schemes also indicate that the positive ZV and ZVD schemes remain robust when applied on continuous systems. And, of course, their performances become even better when the system is effectively SDOF, because then there is only one dominant vibration frequency to be suppressed. To conclude this paper, let us point out again that special caution has to be exercised when one attempts to apply the negative input-shaping schemes to a continuous system. Also, for both SDOF and continuous systems, the ZVD scheme is more tolerant of the detuning-parameter error than the ZV scheme, and therefore would be preferable in practice.

Acknowledgements The authors gratefully acknowledge the R.O.C. (Taiwan) National Science Council for supporting this work through Grants NSC92-2212-E006-122 and NSC93-2212-E006-087.

References

1. Connor JJ (2003) Introduction to structural motion control. Pearson Education, Inc. Upper Saddle River, NJ
2. Singer NC, Seering WP (1989) Design and comparison of command shaping methods for controlling residual vibration. In: Bekey GA (General Chair), Proceedings of the IEEE International Conference on Robotics and Automation. Institute of Electrical and Electronics Engineers, Piscataway, NJ, pp 888–893
3. Singer NC, Seering WP (1990) Preshaping command inputs to reduce system vibration. ASME J Dyn Syst Meas Control 112:76–82
4. Lin T-C (1993) Design an input shaper to reduce operation-induced vibration. In: Haddad AH (General Chair), Proceedings of the 1993 American Control Conference. Institute of Electrical and Electronics Engineers, Piscataway, NJ, pp 2502–2506
5. Jones SD, Ulsoy AG (1994) Control input shaping for coordinate measuring machines. In: Khalil H (General Chair), Proceedings of the 1994 American Control Conference. Institute of Electrical and Electronics Engineers, Piscataway, NJ, pp 2899–2903
6. Singhose WE, Singer NC, Seering WP (1996) Improving repeatability of coordinate measuring machines with shaped command signals. Precision Eng 18:138–146
7. Singhose WE (1997) Command generation for flexible systems. Ph.D. thesis, Department of Mechanical Engineering, Massachusetts Institute of Technology, Cambridge, MA
8. Pao LY, Lau MA (2000) Robust input shaper control design for parameter variations in flexible structures. ASME J Dyn Syst Meas Control 122:63–70
9. Singhose W, Porter L, Kenison M, Kriikku E (2000) Effects of hoisting on the input shaping control of gantry cranes. Control Eng Practice 8:1159–1165
10. Shan J, Liu H-T, Sun D (2005) Modified input shaping for a rotating single-link flexible manipulator. J Sound Vibr 285:187–207

11. Yang T-S, Chen K-S, Lee C-C, Yin J-F (2006) Suppression of motion-induced vibration of a cantilever beam by input shaping. J Eng Math 54:1–15
12. van Kessel PF, Hornbeck LJ, Meier RE, Douglass MR (1988) MEMS-based projection display. Proc IEEE 86:1687–1704
13. Yang T-S, Liang W-L (2003) Suppression of nonlinear forced waves by input shaping. Wave Motion 37: 101–117
14. Su S-P, Yang T-S (2002) Suppression of nonlinear forced waves by error-insensitive input shaping. J Chinese Soc Mech Eng 23:507–516
15. Chen K-S, Yang T-S, Yin J-F, Chen J-Y (2006) Residual vibration suppression for Duffing nonlinear systems with electromagnetic actuation using nonlinear input shaping techniques. ASME J Vibr Acoust (to appear)
16. Chen K-S, Yin J-F, Yang T-S, Ou K-S (2004) Residual vibration suppression of a piezoelectrically driven cantilever beam by input shaping. J Chinese Soc Mech Eng 25:59–67
17. Yamamoto M, Aizawa S, Higashino M, Toyama K (2001) Practical applications of active mass dampers with hydraulic actuator. Earthquake Eng Struct Dyn 30:1697–1717
18. Zhang Y, Pota HR, Agrawal SK (2002) Modification of residual vibrations in elevators with time-varying cable lengths. In: Rhinehart RR (General Chair), Proceedings of the 2002 American Control Conference. Institute of Electrical and Electronics Engineers, Piscataway, NJ, pp 4962–4966
19. Timoshenko S, Young DH, Weaver W Jr (1974) Vibration problems in engineering, 4th edn. Wiley, New York
20. Churchill RV, Brown JW (1990) Complex variables and applications, 5th edn. McGraw-Hill, New York
21. Churchill RV, Brown JW (1978) Fourier series and boundary value problems, 3rd edn. McGraw-Hill, New York